Journal of King Saud University – Engineering Sciences 32 (2020) 378–387

Contents lists available at ScienceDirect

Journal of King Saud University – Engineering Sciences

journal homepage: www.sciencedirect.com

Original article

Teleoperated robotic arm movement using electromyography signal with wearable Myo armband

Hussein F. Hassan, Sadiq J. Abou-Loukh, Ibraheem Kasim Ibraheem *

University of Baghdad, College of Engineering, Department of Electrical Engineering, Al-Jadriyah, 10001 Baghdad, Iraq

ARTICLE INFO

Article history:
Received 13 January 2019
Accepted 12 May 2019
Available online 14 May 2019

Keywords:
Electromyography signal
Myo gesture armband
Pattern recognition
Robotic arm
Due Arduino

ABSTRACT

The primary purpose of this research is to move a 5-DoF Aideepen ROT3U robotic arm in real-time based on the surface Electromyography (sEMG) signal obtained from a wireless Myo gesture armband to distinguish seven hand movements. The pattern recognition system is employed to analyze these gestures and consists of three main parts: segmentation, feature extraction, and classification. Overlap technique is chosen for segmenting portion of the signal. Six-time domain features, namely, Mean Absolute Value (MAV), Waveform Length (WL), Root Mean Square (RMS), Autoregressive Coefficients (AR), Zero Crossings (ZC), Slope Sign Changes (SSC) are extracted from each segment. While the Support Vector Machines (SVM), Linear Discriminant Analysis (LDA), and K-Nearest Neighbor (K-NN) classifiers are employed in the classification of the seven hand movements. Moreover, a comparison between their performance is carried out to obtain optimum accuracy. The proposed system is tested on datasets extracted from six healthy subjects and the results showed that the SVM achieved higher system accuracy with 95.26% compared to LDA with an accuracy of 92.58%, and 86.41% accuracy achieved by K-NN.

1. Introduction

The electrical signal produced through contraction or relaxation of the muscles ruled by the nervous system is called the Electromyography (EMG) signal. This signal depends on the physiological and anatomical characteristic of muscles and is considered to be a complex signal. The surface electromyography (sEMG) is EMG signals that collect the electrical signals of the muscle activity by placing the electrodes on the surface of the skin. Fig. 1 shows the surface electromyography (sEMG) signals that start with the low amplitude and changes with muscle contraction activity (Gheab and Saleem, 2008).

Hand gesture recognition systems usually depend on either visual based detection or internal sensor detection. Visual-based gesture recognition perceived gestures remotely without wearable devices using almost camera. These types of systems typically suffer from many drawbacks such as sensitivity to light, changing distance, hand motion modeling complexity, and position. On the other hand, hand gesture recognition systems based on internal sensor detection (e.g., sEMG signal) which depend on muscle contraction of the hand are more reliable and efficient, thus, it is considered to be one of the distinguishable methods (Bisi et al., 2018). Detection of sEMG signals is useful and improve the essential methodologies in many applications. Such applications are becoming increasingly in demand, such as biomedical engineering (Wang et al., 2017), robotics arm and automation control systems (Gonzalo and Holgado-Terriza Juan, 2015; Pham et al., 2017).

The measurements and precise representations of the sEMG signals depend on the characteristics of the electrodes and their relationship with the skin of the forearm or shoulder and are affected by the amplifier design and the transition of the sEMG signals from analog to digital format (Day, 2002). A raw sEMG signal has the maximum voltage of (0–2) mV, and a range of frequency approximately between (0–1000) Hz. Nonetheless, the vital frequency that contains useful information lies between (20–500) Hz (Ghapanchizadeh et al., 2017). The sEMG signals can be acquired by positioning surface electrodes on the arm or the shoulder.

Two main types of electrodes acquire EMG signals, these are needle electrodes (inside the skin) and surface electrodes, with no significant variance between them (ULKIR et al., 2017). There are two types of surface electrodes, namely, gelled and dry sEMG electrodes. Gelled sEMG electrodes contained a gelled electrolytic

* Corresponding author.
E-mail address: ibraheem.i.k@ieee.org (I.K. Ibraheem).
Peer review under responsibility of King Saud University.

Production and hosting by Elsevier

https://doi.org/10.1016/j.jksues.2019.05.001
1018-3639/

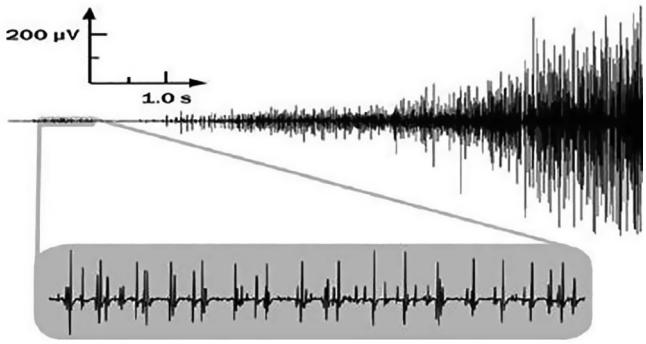

Fig. 1. Estimating the sEMG signal for forearm muscle via a surface electrode (Gheab and Saleem, 2008).

material as an interface between electrodes and the skin. Because of the presence of hair follicles and irregularities in the skin, it is necessary to use gel for conducting with electrodes to reduce the impedance and obtain consistent recordings. The dry electrodes like bar or pin do not require a gel for interfacing and also possible to be in the form of an array (Kilby et al., 2016). Furthermore, there is an additional category of surface electrodes, i.e., wired electrodes, like Myoware muscle sensor and wireless electrodes such as a Myo gesture control armband, which is dry electrodes. They differ in features and more specifically in the sampling rate. All these types of electrodes are considered as data acquisition equipment.

The data acquisition represents the first stage in detecting sEMG signals and recording them, processing them by removing noise and unwanted parts of the signal. The pattern recognition represents the backbone of sEMG signals analysis and processing. To move the assisting devices, such as robotic arms or prosthetic limbs, the pattern recognition system is mostly used to obtain gestures of the muscle activity. It consists of three main stages: segmentation, feature extraction selection, and classification (Naik et al., 2016; Samuel et al., 2018; ULKIR et al., 2017).

In the segmentation stage, the sEMG signals are segmented into slices (windows) or time-slots to extract features for each window, during the muscles' activity. There are two significant points in the segmentation stage, namely, the length of the segment and segment schema; they need to be specified accurately since accuracy is affected by them.

The feature extraction stage is when suitable features are selected to extract information from each window of the sEMG signals. The characteristics of sEMG signals can be categorized by Time Domain (TD), Frequency Domain (FD), and Time-Frequency domain (TF). TD features extraction is easy to implement and does not require a high computational cost. TD features, such as WL, MAV, AR, SSC, ZC, and RMS are extracted from the data that rarely related to the amplitude and frequency of the raw sEMG signals. In contrast, FD features are extracted widely using Power Spectral Density (PSD). The FD features include median frequency, mean power, peak frequency, maximum amplitude and variance of the central frequency. The TF features which depends on TF domain like Wavelet Transform (WT) and Short Time Fourier Transform (STFT) require higher computational cost and are more complex compared to TD features (Ali, 2013; Altın and Er, 2016; Asogbon et al., 2018).

The most appropriate classifier algorithm is chosen in the classification stage. The classifier will determine the intended movement depending on the feature-class sets previously defined. The classifiers are applied to distinguish different sets of features. Many techniques are used for the classification purpose, including well-known algorithms, such as LDA, SVM, K-NN, Artificial Neural Networks (ANN), and fuzzy logic (FL) (Nazmi et al., 2016).

In sEMG signals, there are many applications such as an anthropomorphic prosthetic hand (Wang et al., 2017), an anthropomorphic robot hand (Yang et al., 2009), Control of Home Devices (Gonzalo and Holgado-Terriza Juan, 2015). In addition, there are many applications in the robotic field such as (Murillo et al., 2016; Fukuda et al., 2003; Yoshikawa et al., 2007).

Many studies have been conducted in the literature for the study and analysis of the sEMG signal, most of them depend on wired sEMG electrode as an acquisition system with the high sampling rate (De et al., 2010; Chowdhury et al., 2013). Such custom acquisition system design faces high signal noise and difficulties in selecting suitable placement and the electrode internal distance. The current work-study depends on Myo gesture armband which is a low-cost generic design, wearable, multi-channels with built-in filters to reduce noises.

Other studies used Myo gesture armband with custom design classifiers such as Fuzzy, ANN, and Neuro-Fuzzy approaches (Ahsan et al., 2011; Khezri et al., 2007; ULKIR et al., 2017). The SVM classifier used in this study has a similar performance to that of the Neuro-Fuzzy one and outperforms the fuzzy and ANN classifiers. The system proposed in (Krishnan et al., 2017) used the Linear SVM classifier with the frequency domain features to classify five hand gestures. In this study, the same classifier is adopted, but with Gaussian kernel and TD features that has a low computational cost and easy to implement, more especially in real time.

The primary motivation of this study is to replace the wired electrodes used for sEMG signal with the wireless Myo gesture armband for the aim of moving a 5-DoF Aideepen ROT3U robotic arm in real-time. This replacement will add more free and comfortable for hand movement of the subject. Also, the Myo armband is generally less expensive than other sEMG sensors. The Myo might be a practical substitution for progressively costly gadgets utilized beforehand.

The contribution of the paper is present the best parameters of the pattern recognition system to distinguish seven hand gestures (wrist right, wrist left, wrist up, wrist down, fist, resting hand, and open hand), which give high system performance in order to move the robotic arm in real-time. The parameters such as the number of channels and window size affect the system accuracy and delay time, the effective features extraction used, and suitable classifiers to such type of datasets.

The structure of this paper is as follows: Section 2 describes the background and some theoretical principles of data acquisition and pattern recognition system. Section 3 explains the suggested sEMG signal based methodology to move a 5-DoF Aideepen ROT3U robotic arm in real-time. The experiments in offline mode and online mode are presented in Section 4. Section 5 explores the simulation results and the comparisons between the performance of the different classifiers. Finally, the paper is concluded in Section 6.

2. Theoretical Background

The Myo gesture control armband is a wireless wearable technology designed by Thalmic Labs in 2014 with five gestures of the hand. It has three parts: gyroscope, accelerometer, and magnetometer. Each part contains the three axes of x, y, z, and all these parts represent the Inertial Measurement Unit (IMU). The Myo gesture armband includes two battery cells in different locations; each cell has a capacity of 260 mA/hr and an operating voltage range of 1.7 to 3.3 V. The sampling frequency of Myo gesture control armband is 200 Hz (Mahmoud Abduo and Galster, 2015; Mannion, 2016). It is mainly used for medical purposes, automation systems applications, and to control robotic arms and Unmanned Arial vehicles (UAV). Moreover, this product is supported by the SDK

kit, which enables communication between Myo gesture armband and other software applications, such as MATLAB.

In the segmentation section, there are many approaches used to cut off the sEMG signals, such as adjacent and overlap schemes. The segmentation scheme adopted in this paper is the overlapping scheme. This type of segmentation divides the sEMG signals into regular time slot windows which overlap with each other. Classification Decision (CD) in the overlap technique can be calculated as:

$$CD = \frac{1}{2}T_a + \frac{1}{2}T_{new} + \tau \quad (1)$$

where T_a represents window length, T_{new}represents window increment and τ represents processing time (Ali, 2013; Nazmi et al., 2016). Furthermore, in this research, six TD features are extracted for each window, these are, RMS, MAV, SSC, ZC, AR, and WL.

In the following, the symbols $\boldsymbol{f_k}$ represents the sEMG signal in each segment, and N is the number of samples of the sEMG signal. The informative data that each feature represents is as follows (Ali, 2013; Huang et al., 2016):

1- *Root Mean Square (RMS)*: It has frequency related features, which is the square root of the mean square of the segment. The mathematical representation of RMS is,

$$RMS = \sqrt{\frac{1}{N}\sum_{K=1}^{N} f_k^2} \quad (2)$$

2- *Mean Absolute Value (MAV):* It has amplitude related features, which is found by calculating the mean absolute value of the segment. The mathematical representation of MAV is,

$$MAV = \frac{1}{N}\sum_{K=1}^{N-1} |f_k| \quad (3)$$

3- *Slope Sign Changes (SSC):* It has frequency related features, which detect changes in the slope sign of the sEMG signal and count them. The mathematical representation of SSC is as expressed as,

$$SSC = \sum_{k=2}^{n-1} |(f_k - f_{k-1})(f_k - f_{k+1})| \quad (4)$$

4- *Waveform Length (WL):* It has amplitude related features, which represents the cumulative length of the sEMG waveform over the time segment. The mathematical representation of WL is given as,

$$WL = \sum_{k=1}^{N-1} |f_{k+1} - f_k| \quad (5)$$

5- *Zero Crossings (ZC):* It has frequency related features, which represents counts of how much signal amplitude crosses the zero amplitude over time segment. It is measuring the frequency shift and shows the number of signal sign variations. The mathematical representation of ZC is as follows,

$$ZC = \sum_{k=1}^{N-1} sng(f_k f_{k+1}) \cap |f_k - f_{k+1}| \geq \alpha \quad (6)$$

$$sng(x) = \begin{cases} 1 & if\ x \geq \alpha \\ 0 & otherwise \end{cases}$$

where α is a threshold.

6- *Auto Regression (AR):* This represents the linear combination of previous windows plus the error term. The mathematical representation of AR is,

$$x_n = \sum_{k=1}^{p} a_k f_{n-k} + e_n \quad (7)$$

where $n = 0, 1 \ldots N-1$, a_k is the AR model coefficient, p is the AR model order, e_n is the residual white noise.

The present study adopts three types of well-known classifier algorithms, these are, SVM, LDA, and K-NN. The K-NN process begins at the test point and increases its region until it includes K training samples and applies the majority vote of these samples to identify the test point. The research has shown that no optimal number of neighbors fit all kinds of datasets because each dataset has its requirements (Dougherty, 2013). The SVM is a linear model used to implement non-linear classification boundaries. The support vector classification deduces a computationally efficient path of learning 'good' splitting hyperplanes in dimensional feature space, whereby 'good' hyperplanes could distinguish between new sample classes. In many real-life applications, there are non-separable cases of data when both classes are overlapping. In such a situation, it becomes impossible to split the data with linear separation. Therefore, the SVM maps the data by applying a nonlinear transformation by a suitable selection of basis functions into a higher-dimensional feature space, where the situation becomes linear. There are many kernel functions in the SVM algorithm such as the linear, Radial Basis Function (RBF), polynomial and sigmoid functions (Ali, 2013; Dougherty, 2013). The LDA is Statistical classifier where a new observation should be assigned to mutually exclusive categories. The objective of the LDA, like the SVM technique, is to find a hyperplane that can split the data points into different classes. This hyperplane can be obtained by finding a model which enlarges the distance between the mean of the classes and reduce the variance within the class under the assumption of normal data distribution. The key point of the successful system is how to choose the appropriate features to support the classifier.

The accuracy of the system depends on the number of correct predictions of the classifier divided by the number of total predictions, measured in percentage (Ali, 2013).

$$Accuracy = \frac{No.\ of\ correct\ predection}{Total\ No.of\ predection} \times 100 \quad (8)$$

where the number of correct predictions is the correct output from the compression of predictions class with class testing, while the total prediction is all the expected movements from the classifier.

3. Methodology and hardware components

The system which was designed consists of three main parts: data acquisition, pattern recognition algorithm, and the driven robotic arm. Fig. 2 shows all parts of the proposed system.

3.1. Data acquisition and synchronization

The Myo gesture control armband is used as data acquisition equipment for recording the sEMG signals. It is wireless sEMG electrodes (sensors) that surround the forearm and detect the electrical signals of muscle activities. It consists of eight sEMG stainless steel medical sensors where each sensor represents one channel. It has advantages over other conventional sEMG sensors because no cables are required, free movement, easy to wear, relatively cheap, small in size, and lightweight. Fig. 3 presents the Myo gesture armband.

Eight datasets were recorded of seven gestures for six healthy subjects. Each gesture in the dataset holds for five seconds and starts with a rest hand gesture, thus, the length of each dataset is 35 s. The total dataset recording for each subject is 280 s. The dataset divided into a training set and testing set using a cross-validation technique. In the cross-validation, the original dataset

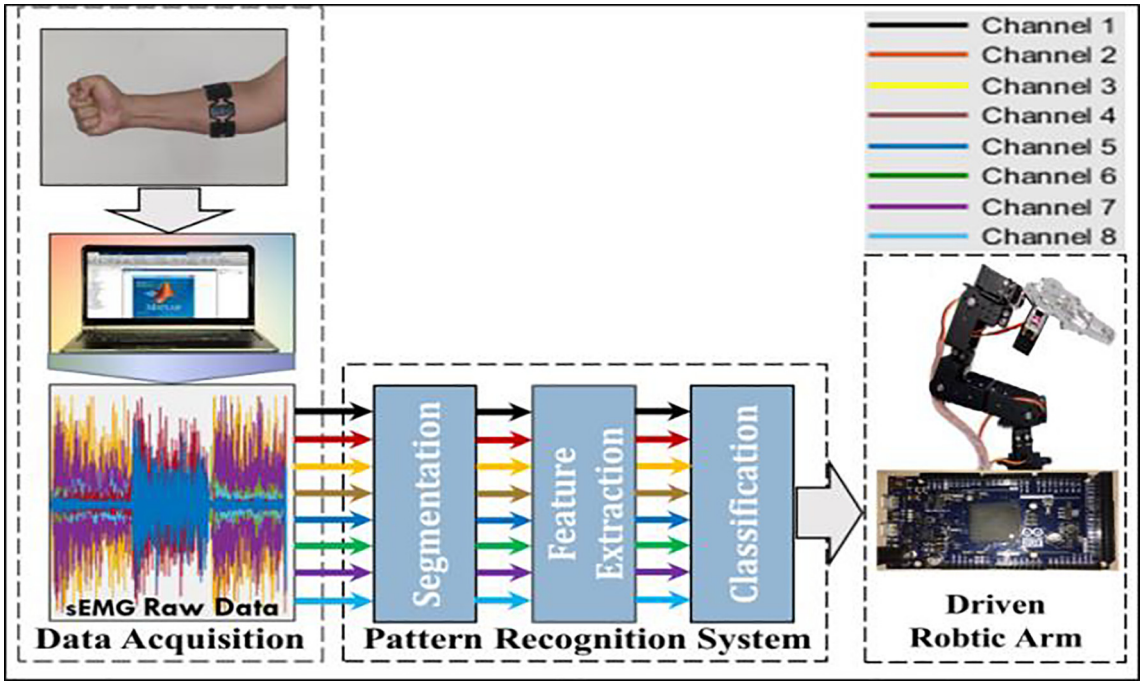

Fig. 2. Block diagram of the overall proposed system.

Fig. 3. Myo gesture armband.

is randomly partitioned into *k* equal sized sub-datasets. A single sub-dataset is retained as the validation data for testing the model, and the remaining sub-datasets are used as training sets. For implementing cross-validation, the recorded datasets partitioned into eight sub-datasets. The information about six healthy subjects in this study is given in Table 1.

Usually, the collected sEMG signals are normally noisy due to ambient noise, motion artifact, inherent noise in electronics equipment, and inherent instability of the sEMG signal. The ambient noise is originated due to the radiation of electromagnetic devices, while the motion artifact noise is caused by the interface between the electrode and the skin. The noise generated by electronic devices, as a result, is called the inherent noise. The intrinsic instability occurs due to the motor units firing rate effects on the sEMG signals. When using the Myo gesture armband, practically the noise ratio in sEMG signals is low and does not affect the sEMG

Table 1
Information about the volunteered subjects.

No. of Subject	Gender	Length (cm)	Weight (Kg)	Age (year)	Hand side
Subject 1	Male	185	128	47	Right
Subject 2	Male	190	97	44	Right
Subject 3	Female	165	72	43	Right
Subject 4	Female	165	80	37	Right
Subject 5	Male	178	100	36	Right
Subject 6	Female	165	63	25	Right

data. Normally, the sEMG signal voltage is minimal, about (0–2) mV, the Myo gesture armband amplifies the sEMG signals so that they can be easily handled.

3.2. Pattern recognition system

The pattern recognition system consists of three stages, as illustrated in Fig. 2. It is used to analyze and process the sEMG signals to distinguish seven hand gestures, namely, wrist right, wrist left, wrist up, wrist down, fist, open hand, and rest hand, as shown in Fig. 4

3.2.1. Segmentation

The window length of sEMG signals plays a vital role in classification accuracy and the required time to process sEMG signals in online-mode. When the window length is relatively small, the classification accuracy will be low, because the information is highly distorted. As a consequence, it is difficult to extract useful information from each window. In contrast, if the window length gradually increases, the delay time will also increase, as well as the classification accuracy, to a certain degree, beyond that there will be no increase in the system accuracy. Therefore, a trade-off between the accuracy and delay time should be balanced to guarantee high accuracy and low delay time. In this work, the overlap segmentation technique is adopted in this study and practically selected window size 240 ms and window increment 120 ms were used for each dataset.

3.2.2. Feature extraction

After segmentation of the sEMG signals into windows of equal size, specific features that are extracted from each window of sEMG signals are selected. These features types will guarantee a high accuracy of separation gestures. Information cannot be obtained for features from individual samples of the sEMG signals.

In this paper, the time domain features, i.e., MAV, RMS, WL, AR, ZC, and SSC are selected due to their ease of implementation and do not need high computational resources. These features are extracted from each window for each channel of the sEMG signals, resulting in a matrix of features. The number of the rows of the matrix represents the total number of windows of the sEMG data, while the number of columns represents the total number of the features for all channels. Table 2 explains feature effectiveness in each channel for each subject of the SVM classifier. The less useful features are preferably deleted to decrease the computational time, especially in real-time. ZC and SSC features have less effect on the classification accuracy, based on that, it is removed from the real-time implementation.

3.2.3. Classification

Three types of classifiers are used in the study, these are, SVM, LDA, and K-NN with K = 7 for comparison to obtain the highest system accuracy among them. The two models of the SVM classifier are implemented; linear and the RBF(Gaussian) models in order to guess the nature of the feature space data. Table 3 shows the results of the models.

From the results in Table 3, the performance of the RBF is better than the linear for SVM classifier, and thus it was concluded that the nature of the data obtained from volunteers is non-linear sep-

Table 3
The results of the SVM gaussian and linear models.

Subject	SVM linear model (%)	SVM RBF model (%)
Subject1	89.6	96.3
Subject2	89.8	95.05
Subject3	91.5	95.57
Subject4	89.3	95.3
Subject5	91.2	95.72
Subject6	87.5	93.66
Average	89.82	95.27

Fig. 4. Seven hand gestures of the proposed system.

Table 2
Feature efficiency (%) for each subject of the SVM classifier.

No. of Subject	RMS	MAV	WL	AR(4)	ZC	SSC
Subject1	96.12	96.55	94.20	72.67	48.67	35.78
Subject2	93.16	93.08	90.24	66.78	50.74	41.71
Subject3	95.80	95.57	92.06	61.86	40.53	29.97
Subject4	94.21	93.41	92.14	64.63	45.96	38.22
Subject5	95.53	95.59	93.47	66.93	45.71	34.16
Subject6	93.56	93.48	91.50	56.22	41.24	31.29
Average	94.73	94.61	92.29	64.85	45.48	35.18

arated. Therefore, the RBF kernel of the SVM classifier was adopted in this study. The RBF function is given as in equation (9) below:

$$K(x_n, x_i) = exp(-\gamma||x_n - x_i||^2 + C) \quad (9)$$

where $K(x_n, x_i), x_n, x_i, \gamma, C$ represent kernel function, support vector data, feature data, gamma, cost of the penalty respectively. To obtain the high system accuracy by SVM classifier, the hyperparameters (γ, C) prefer to be optimum. The iterative method grid search was used to achieve optimum values, where the optimal hyperparameters output of grid search method was C = 9 and gamma = 12.5 (Achirul Nanda et al., 2018).

LDA is a statistical classifier where a new observation should be assigned to mutually exclusive categories. The objective of LDA, like SVM technique, is to find a hyperplane that can split the data points fall in different classes. The Linear discriminant analyses based on the Bayes classification rule.

$$P(C_k|X) = \frac{P(C_k)P(x|C_k)}{P(x)} \quad (10)$$

where $P(C_k|X)$ is the probability density function for the test vector within k class,$P(C_k)$ is the previous probability for class k and usually presumed to be equal for all classes, and $P(x)$ is the probability density function of the training space and is also assumed to be equal for all classes (Zhang et al., 2013).

The K-NN classifier determines the class of (x) test data point based on the nearest training points (K) to it and classifies it to the classes that have the most probability. The K-NN process begins at the test point and increases a region until it includes (K) training samples and applies the majority vote on these samples to identify the test point (x). The probability density function P(X, C_j), for the characteristic data X, presented class C_j is defined as follows:

$$P(X, C_j) = \sum_{d_i \in KNN} Sim(X, d_i).y(d_i, C_j) \quad (11)$$

where C_j represents training classes, and X represents the feature vector of the test data. Also, a d_i is one of the neighbors in the training set, y (d_i, C_j)∈{0,1} means if d_i belongs to category C_j, and $Sim(X, d_i)$ is the similarity function for X and d_i (Kim et al., 2011).

The prediction of the classifier would be applied in the next stage as commands to move the robotic arm. If any channel has low efficiency and has little effect on the overall accuracy of the system, it can be removed to gain reduce the computational time, thus, speeding up the system response especially in real-time mode, as in the case of channel 2. Table 4 shows that channel two has a little effect on the accuracy of different subjects as compared with other channels. Where the dataset for each subject represents all gestures for each channel, which are (wrist right, wrist left, wrist up, wrist down, fist, open hand, and rest hand as shown in Fig. 4) which is repeated eight times.

4. System modes

The system works in two modes: *offline mode* and *online mode* (real-time). The offline mode is developed for calculating system accuracy and improving system performance, while the online mode is used for moving the robotic arm in real time. These two modes have been implemented through the MATLAB R2017 program.

4.1. Offline mode

The Myo gesture armband should be worn in the same manner at every time it is used to record the datasets to guarantee the placements of its sensors in the same position. To avoid random readings, this point must be considered during data recording. In this study, the Myo armband is worn on the right forearm, as shown in Fig. 5.

Myo gesture armband is used in this study to collect raw sEMG signals from all channels during muscle contraction activity. The information acquired by Myo armband is transmitted to the computer via Bluetooth for analysis and processing in MATLAB R2017 environment. The duration of the recording dataset is 280s. The window size in the dataset is 240 ms with 120 ms overlapping. The number of features extracted for each set for all channels is 72, which equals to the number of Myo channels (eight channels) multiplied by the number of features (six features: RMS, MAV, SSC, ZC, WL, and AR with order = 4) per window (segment).

Three vectors are calculated in addition to the dataset; the first vector is a feature vector composed of six features extracted from each window for each channel. While the second vector is a class vector representing the movements of the dataset.

Finally, the third vector is an index vector representing the index of starting the movement in the dataset. Proper synchronization between class vector and index vector improves movement classification accuracy. For the best synchronization, the programmable model was developed to improve the accuracy of the system.

The accuracy of the system is calculated as in equation (8). The accuracy of the system using this procedure with the K-NN classifier was 86.41%, while it was 92.58% with LDA classifier, and 95.26% with SVM classifier.

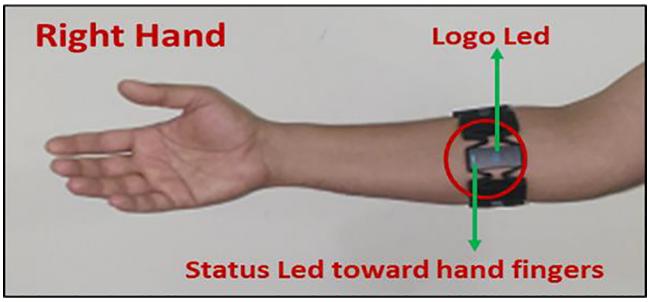

Fig. 5. The manner of wearing Myo gesture armband.

Table 4
Accuracy results of the six extracted feature per channel with SVM classifier.

No. of Subject	Ch1	Ch2	Ch3	Ch4	Ch5	Ch6	Ch7	Ch8
Subject1	63.02	45.97	62.58	73.38	71.75	55.21	56.07	56.40
Subject2	52.94	39.13	41.84	57.15	47.75	57.33	55.57	57.34
Subject3	58.04	37.18	47.64	45.22	48.71	46.12	52.95	68.44
Subject4	60.22	40.84	52.17	56.06	58.51	51.67	51.88	67.45
Subject5	64.40	64.47	48.31	51.25	65.45	69.84	37.47	59.57
Subject6	54.60	51.75	46.85	53.54	61.71	45.82	42.85	62.43
Average	58.87	46.56	49.90	56.1	58.98	54.33	49.47	61.94

4.2. Online mode

In the real-time mode, the 5-DoF Aideepen ROT3U robotic arm, Due Arduino microcontroller, HP laptop computer, and Myo gesture armband comprise the hardware components of the entire system. The Aideepen ROT3U robotic arm has a rotation angle of 180 degrees, a height of 42 cm (holder closed), clamp the maximum opening of 4.5 cm, and widest distance of the holder of 10 cm. It consists of five servo motors type MG 996R; each servo motor has an operating voltage of 4.8 V to 7.2 V, with running current of 500 mA–900 mA (6 V), operating speed: 0.17 60°/s (4.8 V), 0.14 60°/s (6 V), and torque: 9.4 kgf-cm (4.8 V), 11 kgf-cm (6 V). Due Arduino specifications are: operating voltage: 3.3 V, digital I/O pins: 54 (of which 12 provide PWM output), analogue input pins: 12, DC current for 5 V pin: 800 mA, flash memory: 512 KB all available for the user applications, SRAM: 96 KB (two banks: 64 KB and 32 KB), and clock speed: 84 MHz. HP laptop computer specifications are Processor: Core i5–2.3 GHz, RAM: 8 GB. Fig. 6 shows the Due Arduino and the robotic arm.

To move the robotic arm like a human arm movement, the data collected by Myo armband transmits to the computer via Bluetooth. The pattern recognition algorithm processes these data to predict the intended movements. The output of pattern recognition is a vector of anticipated movements; each value in this vector represents one gesture. The majority vote is applied to this vector to guarantee a smooth movement of the robotic arm. Majority vote produces final movements that have been predicted most frequently by the classifier.

The response time of the robotic arm movement as a result of moving a human arm gesture is an essential factor in the success measurement of the system. To improve the system response, delay time should be reduced. There are many types of delay time in the system, such as Bluetooth transfer delay, the computational time of pattern recognition, and Arduino processing time. Bluetooth transfer delay could not be reduced, because it is a standard protocol used by the manufacturing company of Myo gesture armband. The computational time of pattern recognition can be reduced depending on offline mode results; therefore, it is possible to delete factors that do not significantly affect accuracies, such as channel 2, and the ZC and SSC features.

The clock speed of Arduino (microcontroller) plays an essential role in processing time, therefore, to improve the response time of the system, it is better to select a high clock speed for Arduino. Early experiments used UNO Arduino, which has a clock speed of 16 MHz. Then it was replaced by DUE Arduino that has a clock speed of 84 MHz to reduce delay time and also to improve the response time of the robotic arm. In this mode, the testing set acquired from the Myo armband is directly cut off into segments, and the feature testing is calculated for these segments. Furthermore, in the classification stage, the classifier expects the predicted vector. The majority vote is applied and passes each value from it to the Arduino, which is connected by a serial port to the computer to move the robotic arm.

5. Results and discussion

This section discusses the results of experiments and factors that affect the accuracy of the system. The influential factors are the length of the window, type of the features selected and classifier, and the number of influencing channels in the Myo armband.

5.1. Experiment one: effect of window length on system accuracy

The length of the sEMG signal segment affects the accuracy of the classification and the delay time of the system, as explained previously in the segmentation section. In this experiment the window size changes from 100 to 750 ms. During the duration between (100–500) ms, the accuracy of classification increases significantly, but during the period between (500–750) ms, increasing window size does not lead to a noticeable increase in accuracy. The window size of the system should be kept below 300 ms of the sample rate because of considerations of the real-time constraint, where the output response time should not exceed this period which represents the time of the processing of classification decisions (Englehart and Hudgins, 2003; Hargrove et al., 2007). The best results were obtained when the window size is 240 ms through a trade-off between system accuracy and delay time. Fig. 7 shows the relationship between system accuracy and window length.

5.2. Experiment two: effect of extracting feature selection on system accuracy

Feature selection is essential to extract information from sEMG signals because the classifier can distinguish between movements based on the extracted information of these features. In this experiment, the average accuracy of the system was 95.26%, 92.58%, and 86.41% for SVM, LDA, and K-NN respectively, for six features

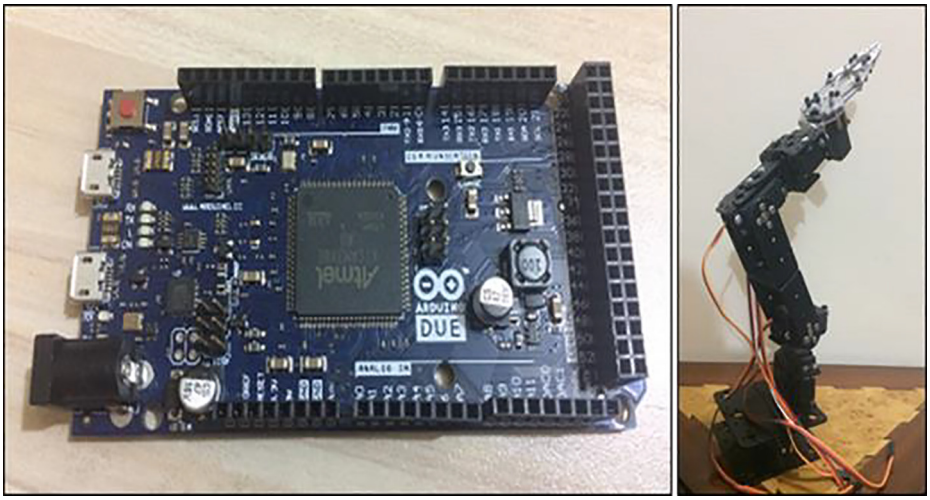

Fig. 6. Due Arduino microcontroller and 5-DoF Aideepen ROT3U aluminum robotic arm.

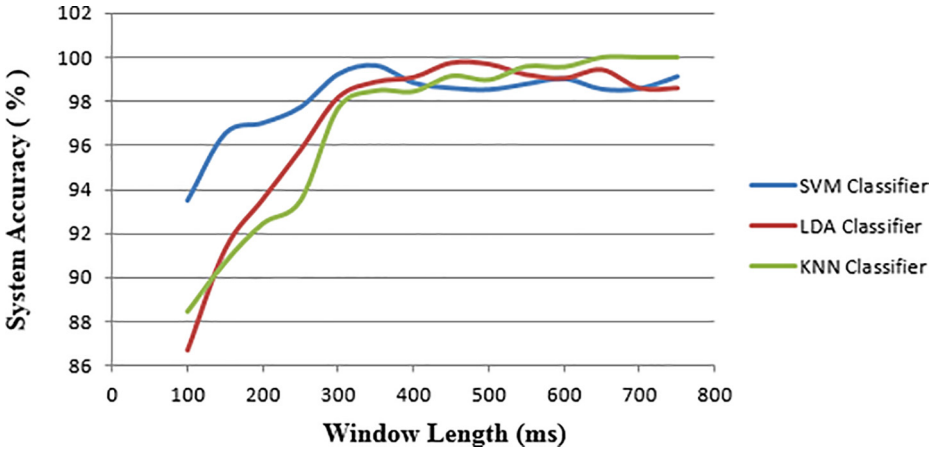

Fig. 7. Effects of the window length on system accuracy with three classifiers.

extracted and eight channels for six subjects. By observing offline results in Table 2, the RMS feature had a high effect on the accuracy of the system, but the ZC and SSC features had little impact on the system's accuracy. Therefore, these features can be removed from the feature vector set to reduce computational cost and hence minimizing processing time. Thus, online mode depended mainly on four features: AR, WL, RMS, and MAV.

5.3. Experiment three: effect of the number of channels on system accuracy

Some of the Myo armband sensors will be positioned on muscles that have a little electrical activity which will impact on the value of information collected from that sensor. Therefore, by observing offline results, it was apparent that channel two had the poorest impact on the accuracy of the system for most subjects. Therefore, to minimize the computational cost, this channel can be removed from the pattern recognition system. Thus, in the online mode, seven channels instead of eight channels are considered. Tables 5 and 6 explain the accuracy of the system before and after removal of the ZC and SSC features, and channel 2.

Fig. 8 shows the confusion matrix while training the SVM classifier on the subject data when extract RMS, MAV, WL, AR(4) feature set for seven channels (1,3,4,5,6,7,8). From examining the confusion matrix in Fig. 8, the gestures (Up and Right) and (Open and Fist) have the highest error rate. In general, the other gestures have a little correlation between them as illustrated in the figure below.

The comparison of the results of this study in offline mode with other studies is shown in Table 7. Each study in Table 7 has its environmental conditions and differs in many aspects with the others, such as the number and type of subjects, data acquisition approach, the extent of overlap and convergence between classified movements as well as the main differences listed in Table 7 such as feature selection and classifier type. From Table 7, it can be noticed that the SVM classifier with different features domains achieved the best results as well as Neuro-Fuzzy classifier.

Table 5
Accuracy of the system before the removal of the ZC and SSC features, and Channel two for each subject.

No. of Subject	SVM + TD	LDA + TD	K-NN + TD
Subject 1	96.3	91.7	92.1
Subject 2	95.05	93.49	86.29
Subject 3	95.57	94.0	82.36
Subject 4	95.29	94.38	84.09
Subject 5	95.72	94.05	89.9
Subject 6	93.65	87.82	84.52
Average	95.26	92.58	86.41

Table 6
Accuracy of the system after the removal of the ZC and SSC features, and Channel two for each subject.

No. of Subject	SVM + TD	LDA + TD	K-NN + TD
Subject 1	96.08	90.58	91.25
Subject 2	95.60	93.20	88.36
Subject 3	94.25	92.67	86.51
Subject 4	95.44	93.85	85.86
Subject 5	92.15	90.98	84.93
Subject 6	93.33	87.15	86.06
Average	94.48	91.41	87.16

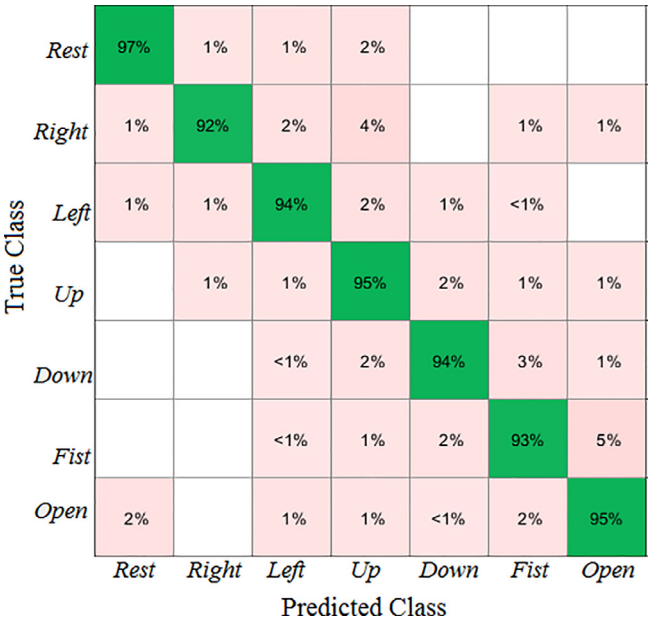

Fig. 8. A Confusion matrix of seven gestures classified.

Table 7
Performance comparison with other studies in offline mode.

No.	Gestures	Sample Rate	Win_size (samples)	Features Extractions	Classifier	Accuracy (%)	Refs.
1	5	200 Hz	50	SSI, Max. frequency, Min. frequency, Mean Power, Mean Frequency,	SVM	92.4	(Krishnan et al., 2017)
2	17	200 Hz 1000 Hz	50 250	MAV, WL, ZC, and SSC	SVM	96.8 99.1	(Phinyomark et al., 2018)
3	6	1000 Hz	200	MAV, SSC, ZC, AR + WT	Neuro-Fuzzy	96.0	(Khezri et al., 2007)
4	16	200 Hz	Disjoint	Wavelet - level4	ANN	89.0	(Luh et al., 2016)
5	5	200 Hz	00	MAV, RMS, VAR, STD,	Feedforward Neural Networks (FNN) SVM	54.0 92.0	(Morales and Cepeda, 2017)
6	9	200 Hz 2 KHz	200	WL, MAV, WAMP, SSC, ZC, Cardinality(CARD)	LDA	91.95 94.18	(Mendez et al., 2017)
7	5	200 Hz	50	Dynamic time warping (DTW)	K-NN, K = 5	86.0	(Benalcazar et al., 2017)
8	7	200 Hz	48	MAV, RMS, WL, AR(4), ZC, SSC	SVM LDA K-NN (K = 7)	95.26 92.58 86.41	This Study

6. Conclusion

A model proposed in this paper is to move the robotic arm (5-DoF) in real-time depends on recognizing human forearm gestures based on sEMG signals collected by wireless Myo gesture armband. The wireless Myo gesture armband added more flexibility and free movement for the system and processes the sEMG signals efficiently. Also, an excellent result was obtained in recognizing patterns using a combination of the overlap segmentation technique, (WL, AR, MAV, and RMS) extract features for each segment and the SVM classifier. Also, the experiment has shown that the size of the window plays an influential role in the accuracy of the system. It can be concluded that the best results were achieved with the SVM and LDA classifiers, while the K-NN classifier achieved acceptable results.

For future research in this field, a recommendation would be to collect more data of volunteers of able and disable-bodied is necessary to draw a robust conclusion about the accuracy of the system. Also, adding one of the control design methods such as (Abdul-Adheem and Ibraheem, 2016; Ibraheem and Abdul-Adheem, 2016) to add more smoothness to the robotic arm movement.

Declaration of Competing Interest

The authors declare that they have no conflict of interest.

References

Abdul-Adheem, W.R., Ibraheem, I.K., 2016. Improved sliding mode nonlinear extended state observer based active disturbance rejection control for uncertain systems with unknown total disturbance. Int. J. Adv. Comput. Sci. Appl. 7, 80–93. https://doi.org/10.14569/IJACSA.2016.071211.

Abduo, Mahmoud, Galster, M., 2015. Myo gesture control armband for medical applications. Dep. Comput. Sci. Softw. Eng. Univ. Canterbury, 4–23.

Achirul Nanda, M., Boro Seminar, K., Nandika, D., Maddu, A., 2018. A comparison study of kernel functions in the support vector machine and its application for termite detection. Information 9, 1–14.

Ahsan, M.R., Ibrahimy, M.I., Khalifa, O.O., 2011. Electromygraphy (EMG) Signal Based Hand Gesture Recognition Using Artificial Neural Network (ANN). In: 2011 4th International Conference on Mechatronics (ICOM). IEEE, Kuala Lumpur, Malaysia, pp. 1–6.

Ali, A.H., 2013. An Investigation of Electromyographic (EMG) Control of Dextrous Hand Prostheses for Transradial Amputees. Plymouth Univ. University of Plymouth.

Altın, C., Er, O., 2016. Comparison of different time and frequency domain feature extraction methods on elbow gesture's EMG. Eur. J. Interdiscip. Stud. 2 (3), 35–44.

Asogbon, M.G., Samuel, O.W., Geng, Y., Chen, S., Mzurikwao, D., Fang, P., Li, G., 2018. Effect of window conditioning parameters on the classification performance and stability of EMG-based feature extraction methods. In: 2018 IEEE International Conference on Cyborg and Bionic Systems (CBS). IEEE, Shenzhen, China, pp. 576–580.

Benalcazar, M.E., Jaramillo, A.G., Jonathan, Zea, A., Paez, A., Andaluz, V.H., 2017. Hand gesture recognition using machine learning and the Myo Armband. In: 2017 25th European Signal Processing Conference (EUSIPCO). IEEE, Kos, Greece, pp. 1075–1079.

Bisi, S., De Luca, L., Shrestha, B., Yang, Z., Gandhi, V., 2018. Development of an EMG-controlled mobile robot. Robotics 7 (3), 36. https://doi.org/10.3390/robotics7030036.

Chowdhury, R.H., Reaz, M.B.I., Ali, M.A.B.M., Bakar, A.A.A., Chellappan, K., Chang, T. G., 2013. Surface electromyography signal processing and classification techniques. Sensors 13 (9), 12431–12466.

Day, S., 2002. Important Factors in Surface EMG Measurement. General White Paper.

De, Carlo J., Luca, B., Gilmore, L.D., Kuznetsov, M., Roy, S.H., 2010. Filtering the surface EMG signal: movement artifact and baseline noise contamination. J. Biomech. 43 (8), 1573–1579.

Dougherty, G., 2013. Pattern Recognition and Classification. Springer, New York, New York, NY.

Englehart, K., Hudgins, B., 2003. A robust, real-time control scheme for multifunction myoelectric control. IEEE Trans. Biomed. Eng. 50 (7), 848–854.

Fukuda, O., Tsuji, T., Kaneko, M., Otsuka, A., 2003. A Human-assisting manipulator teleoperated by EMG signals and arm motions. IEEE Trans. Robot. Autom. 19 (2), 210–222.

Ghapanchizadeh, H., Ahmad, S.A., Ishak, A.J., Al-Quraishi, M.S., 2017. Review of surface electrode placement for recording electromyography signals. Biomed. Res. (Special Issue), 1–7

Gheab, N.H., Saleem, S.N., 2008. Comparison study of electromyography using wavelet and neural network. Al-Khwarizmi Eng. J. 4 (3), 108–119.

Gonzalo, P., Holgado-Terriza Juan, A., 2015. Control of home devices based on hand gestures. In: 2015 IEEE 5th International Conference on Consumer Electronics - Berlin (ICCE-Berlin). IEEE, Berlin, Germany, pp. 510–514.

Hargrove, L.J., Englehart, K., Hudgins, B., 2007. A comparison of surface and intramuscular myoelectric signal classification. IEEE Trans. Biomed. Eng. 54 (5), 847–853.

Huang, H., Li, T., Bruschini, C., Enz, C., Koch, V.M., Antfolk, C., 2016. EMG Pattern Recognition Using Decomposition Techniques for Constructing Multiclass Classifiers 1296–1301.

Ibraheem, I.K., Abdul-Adheem, W.R., 2016. On the improved nonlinear tracking differentiator based nonlinear PID controller design. Int. J. Adv. Comput. Sci. Appl. 7 (10), 234–241. https://doi.org/10.14569/IJACSA.2016.071032.

Khezri, M., Jahed, M., Sadati, N., 2007. Neuro-fuzzy surface EMG pattern recognition for multifunctional hand prosthesis control. In: 2007 IEEE International Symposium on Industrial Electronics. IEEE, Vigo, Spain, pp. 269–274. https://doi.org/10.1109/ISIE.2007.4374610.

Kilby, J., Prasad, K., Mawston, G., 2016. Multi-channel surface electromyography electrodes: a review. IEEE Sens. J. 16 (14), 5510–5519.

Kim, K.S., Choi, H.H., Moon, C.S., Mun, C.W., 2011. Comparison of K-nearest neighbor, quadratic discriminant and linear discriminant analysis in classification of electromyogram signals based on the wrist-motion directions. Curr. Appl. Phys. 11 (13), 740–745. https://doi.org/10.1016/j.cap.2010.11.051.

Krishnan, K.S., Saha, A., Ramachandran, S., Kumar, S., 2017. Recognition of human arm gestures using Myo armband for the game of hand cricket. In: 2017 IEEE International Symposium on Robotics and Intelligent Sensors (IRIS). IEEE, Ottawa, ON Canada, pp. 389–394.

Luh, G.-C., Ma, Y.-H., Yen, C.-J., Lin, H.-A., 2016. Muscle-gesture robot hand control based on sEMG signals with wavelet transform features and neural network classifier. In: 2016 International Conference on Machine Learning and Cybernetics (ICMLC). IEEE, Jeju, South Korea, pp. 627–632. https://doi.org/10.1109/ICMLC.2016.7872960.

Mannion, P., 2016. Myo armband : Wearables Design Focuses On Packaging 10.

Mendez, I., Hansen, B.W., Grabow, C.M., Smedegaard, E.J.L., Skogberg, N.B., Uth, X.J., Bruhn, A., Geng, B., Kamavuako, E.N., 2017. Evaluation of the Myo armband for the classification of hand motions. In: 2017 International Conference on

Rehabilitation Robotics (ICORR). IEEE, London, UK, pp. 1211–1214. https://doi.org/10.1109/ICORR.2017.8009414.

Morales, L., Cepeda, J., 2017. Feature Extraction from sEMG of Forearm Muscles, Performance Analysis of Neural Networks and Support Vector Machines for Movement Classification. In: Proceedings of the 14th International Conference on Informatics in Control, Automation and Robotics. SCITEPRESS - Science and Technology Publications, Madrid, Spain, pp. 254–261. https://doi.org/10.5220/0006429402540261.

Murillo, P.U., Moreno, R.J., Avilés, S.O.F., 2016. Individual robotic arms manipulator control employing electromyographic signals acquired by Myo armbands. Int. J. Appl. Eng. Res. 11 (23), 11241–11249.

Naik, G.R., Al-Timemy, A.H., Nguyen, H.T., 2016. Transradial amputee gesture classification using an optimal number of sEMG sensors: an approach using ICA clustering. IEEE Trans. Neural Syst. Rehabil. Eng. 24 (8), 837–846. https://doi.org/10.1109/TNSRE.2015.2478138.

Nazmi, N., Abdul Rahman, M., Yamamoto, S.-I., Ahmad, S., Zamzuri, H., Mazlan, S., 2016. A review of classification techniques of EMG signals during isotonic and isometric contractions. Sensors 16 (8), 1304.

Pham, T.X.N., Hayashi, K., Becker-Asano, C., Lacher, S., Mizuuchi, I., 2017. Evaluating the usability and users' acceptance of a kitchen assistant robot in household environment. In: 2017 26th IEEE International Symposium on Robot and Human Interactive Communication (RO-MAN). IEEE, Lisbon, Portugal, pp. 987–992. https://doi.org/10.1109/ROMAN.2017.8172423.

Phinyomark, A., Khushaba, R.N., Scheme, E., 2018. . Feature extraction and selection for myoelectric control based on wearable EMG sensors. Sensors (Switzerland) 18 (5). https://doi.org/10.3390/s18051615. 1615,1–17.

Samuel, O.W., Zhou, H., Li, X., Wang, H., Zhang, H., Sangaiah, A.K., Li, G., 2018. Pattern recognition of electromyography signals based on novel time domain features for amputees' limb motion classification. Comput. Electr. Eng. 67, 646–655. https://doi.org/10.1016/j.compeleceng.2017.04.003.

Ulkir, O., Gokmen, G., Kaplanoglu, E., 2017. EMG signal classification using fuzzy logic. Balk. J. Electr. Comput. Eng. 5 (2), 97–101. https://doi.org/10.17694/bajece.337941.

Wang, N., Lao, K., Zhang, X., 2017. Design and myoelectric control of an anthropomorphic prosthetic hand. J. Bionic Eng. 14 (1), 47–59.

Yang, D., Zhao, J., Gu, Y., Wang, X., Li, N., Jiang, L., Liu, H., Huang, H., Zhao, D., 2009. An anthropomorphic robot hand developed based on underactuated mechanism and controlled by EMG signals. J. Bionic Eng. 6 (3), 255–263. https://doi.org/10.1016/S1672-6529(08)60119-5.

Yoshikawa, M., Mikawa, M., Tanaka, K., 2007. A myoelectric interface for robotic hand control using support vector machine. In: 2007 IEEE/RSJ International Conference on Intelligent Robots and Systems. IEEE, San Diego, CA, USA, pp. 2723–2728.

Zhang, Haoshi, Zhao, Yaonan, Yao, Fuan, Lisheng, Xu., Shang, Peng, Li, Guanglin, 2013. An adaptation strategy of using LDA classifier for EMG pattern recognition. In: 2013 35th Annual International Conference of the IEEE Engineering in Medicine and Biology Society (EMBC). IEEE, Osaka, Japan, pp. 4267–4270.